

THERMAL PERFORMANCE OF THE S1-GLOBAL CRYOMODULE FOR ILC

N. Ohuchi[#], M. Akemoto, S. Fukuda, K. Hara, H. Hayano, N. Higashi, E. Kako, Y. Kojima, Y. Kondo, T. Matsumoto, S. Michizono, T. Miura, H. Nakai, H. Nakajima, K. Nakanishi, S. Noguchi, T. Saeki, M. Satoh, T. Shidara, T. Shishido, T. Takenaka, A. Terashima, N. Toge, K. Tsuchiya, K. Watanabe, S. Yamaguchi, A. Yamamoto, Y. Yamamoto, K. Yokoya,
KEK, Tsukuba, Japan

A. Bosotti, C. Pagani, R. Paparella, P. Pierini, INFN, Milano, Italy

T. Arkan, S. Barbanotti, H. Carter, M. Champion, A. Hocker, R. Kephart, J. Kerby, D. Mitchell, Y. Pischnalnikov, M. Ross, T. J. Peterson, FNAL, Chicago, U.S.A

D. Kostin, L. Lilje, A. Matheisen, W. -D. Moeller, N. Walker, H. Weise,
DESY, Hamburg, Germany

Abstract

The S1-Global program was the international research collaboration among INFN, FNAL, DESY, SLAC and KEK as one of the GDE R&D for construction of ILC. The program was successfully completed in March, 2011. As the thermal studies of this cryomodule, the static heat losses at 2K, 5K and 80K were measured and compared with design. The dynamic losses of the DESY, FNAL and two KEK cavities at their maximum operative gradients were measured. In this paper, we will report the summary of the thermal measurements of the S1-G cryomodule.

INTRODUCTION

The S1-Global cryomodule [1, 2] consists of two 6 m cryomodules, as shown in Fig. 1. One was designed by INFN, and it contained two FNAL cavities and two DESY cavities. Most of the associated components, like input couplers and RF cables, were the same as the TTF-III cryomodule [3]. The other was designed by KEK, and the cryomodule contains four KEK cavities. As one of the important studies of the S1-G program, measurement and comparison of thermal performances of these cold components had been proposed. The static heat load and the temperature profiles of the cold components were measured and they were evaluated with respect to the design. The dynamic losses of the DESY, FNAL and two KEK cavities at their maximum operative gradients were obtained by the evaporation of liquid helium (LHe) at 2 K and, the Q_0 values were evaluated. The dynamic losses of input couplers were measured at the same power level as the case of resonant operation at 32 MV/m of the ILC

nominal gradient when the cavities were detuned. These measured data will become important references for the ILC cryomodule and cryogenic design.

THERMAL DESIGN OF CRYOMODULE

The parameters of the Module-A and C in the S1-G cryomodule are listed in Table 1. The total length of the S1-G cryomodule with the end cans was 14.9 m. The cross section designs of Module-A and C were based on the TTF-III cryomodule, as shown in Fig. 2.

The calculated static heat loads of the components are listed in Table 2. The cold components are thermally intercepted with two thermal shields at 5 K and 80 K. The heat loads are calculated with the temperature profiles. In Table 2, the STF-2 input coupler has larger static loss than the TTF-III coupler at each temperature level. This is due to the STF-2 coupler design in order to simplify its assembly inside and outside the clean-room by having no bellows between thermal intercepts of 5 K and 70K.

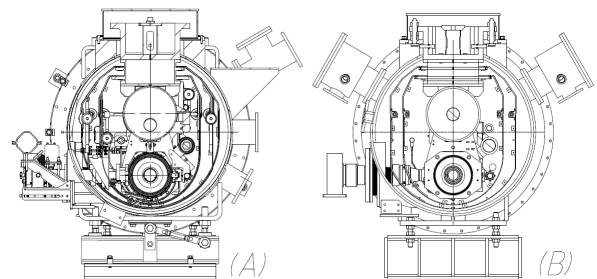


Figure 2: Cross sections of Module-C and -A. Module-C and -A are shown by (A) and (B), respectively.

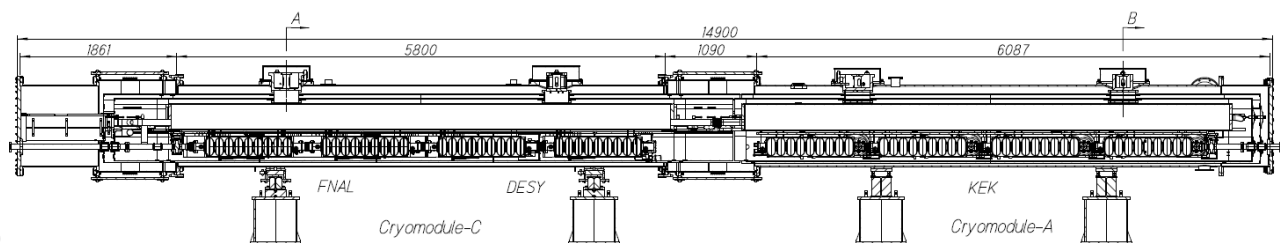


Figure 1: S1-G cryomodule.

Table 1: S1-Global Cryomodule Thermal Parameters

	Module-A by KEK	Module-C by INFN
Vacuum vessel length	6087 mm	5800 mm
Vacuum vessel O.D.	φ965.2 mm	φ965.2 mm
5 K shield cold mass [Al]	185 kg	167 kg
80 K shield cold mass [Al]	210 kg	182 kg
Gas return pipe O.D.	φ318.5 mm	φ312.0 mm
Cavity package	KEK-a/KEK-b	FNAL/DESY
Input coupler	STF-2 type	TTF-III type

Table 2: Static Heat Load at Design

	Cold component	Module-A, W	Module-C, W
2K	Thermal radiation	~0.0	~0.0
	4 input couplers	0.29	0.08
	HOM RF, Piezo cables	2.1	0.71
	4 tuner driving shafts	0.48	NA
	Temp. sensor wires	0.18	0.18
	WPM, Pin diodes wires	1.72	0.82
	WPM connection pipe	0.17	~0.0
	2 support posts	0.25	0.25
	Beam pipe	0.02	<0.01
	Total	5.2	2.1
5K	Thermal radiation	0.66	0.68
	4 input couplers	4.00	0.92
	2 support posts	1.54	1.54
	Beam pipe	0.1	0.05
	Sensor wires	0.9	0.9
	Total	7.2	4.1
80K	Thermal radiation	16.6	15.9
	4 input couplers	9.60	7.28
	2 support posts	10.78	10.78
	RF cables	6.88	1.30
	Beam pipe	0.37	0.10
	Sensor wires	0.08	0.08
	Total	44.3	35.3

STATIC THERMAL MEASUREMENT

The static heat loads at 2 K, 5 K and 80 K were measured by calorimetric methods. The heat load at 2 K was evaluated by measuring the flow rate of evaporated LHe in the 8 cavity vessels. The flow rate was measured at the outlet of the pump unit at room temperature. The heat loads at 5 K and 80 K were calculated by measuring the temperature rises of the thermal shield plates by stopping the LHe and LN₂ flow.

Figure 3 shows thermal conditions of the static heat load measurement at 2 K. The flow rate of evaporated LHe was 6.87 m³/h, and it corresponds to 0.314 g/s. Helium pressure was controlled at 3.14 kPa, and the latent heat of LHe was 23.045 J/g. Therefore, the heat load at 8 vessels is calculated to be 7.2 W. This measured heat load is in good agreement with the estimation given in Table 2, which amounts to 6.8 W if we exclude the contribution of the support posts. The direct heat load from the support posts to the vessels via the gas return pipe is negligible, and its effect is to increase the enthalpy of the evaporated gas rather than to induce additional LHe losses.

07 Accelerator Technology

T13 Cryogenics

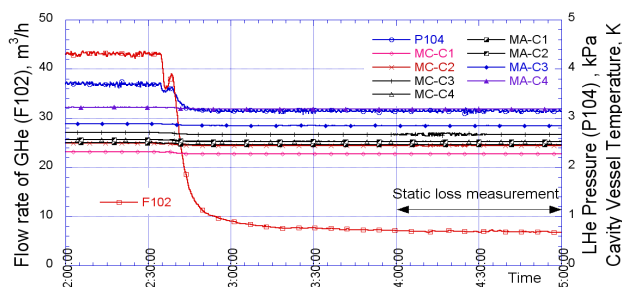


Figure 3: Static loss measurements: flow rate of He=F102, pressure of 2K He=P104, temperatures of cavity vessels =MC-C1~C4, MA-C1~C4. Temperature sensors were attached on the vessel surfaces.

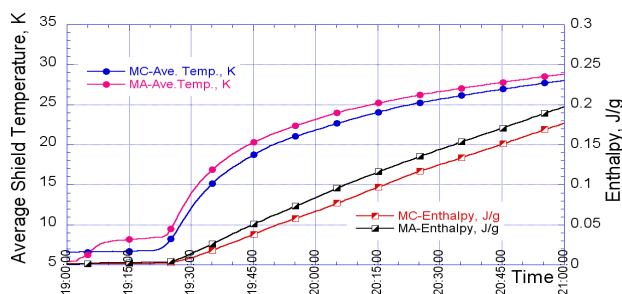


Figure 4: Temperature and enthalpy changes of 5 K shields of Module-A (MA-) and Module-C (MC-).

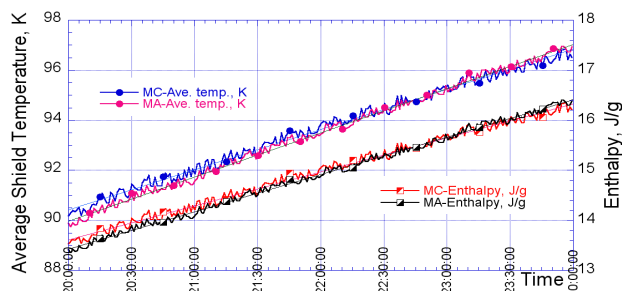


Figure 5: Temperature and enthalpy changes of 80 K shields of Module-A (MA-) and Module-C (MC-).

Figures 4 and 5 show the temperature and enthalpy changes of the 5 K and 80 K shields with time. The temperature profiles of 5 K and 80 K shields were measured by 15 PtCo thermometers and 13 Type-T thermocouples, respectively, for each Module. The plotted temperatures are the average of the measured values. The enthalpies of the shields were calculated from the average temperatures. The heat loads were calculated with the enthalpy increases of the shields, and the measured heat loads are listed in Table 3. The values in parentheses are calculated values in Table 2. The measurement and calculation show a good agreement.

Table 3: Measured Static Heat Load

	Module-A	Module-C
2K	7.2 W [6.8 W]	
5K	7.3 W [7.2 W]	5.3 W [4.1 W]
80K	48.7 W [44.3 W]	34.4 W [35.3 W]

DYNAMIC THERMAL MEASUREMENT

Dynamic Loss by Single Cavity

In order to evaluate the dynamic loss and the Q_0 value at a single cavity, a sequence of four measurements was performed. They were the measurements of the heat loss with a RF operation= Q_{D1} , the corresponding static loss= Q_{S1} , the heat loss at the same power level as the case of resonant operation in the detuned cavity= Q_{D2} and the corresponding static heat loss= Q_{S2} . The dynamic losses at the RF operation and the detuned condition, Q_D and Q_{D-det} , were calculated as follows: $Q_D=Q_{D1} - Q_{S1}$ and $Q_{D-det}=Q_{D2} - Q_{S2}$. The heat loss of Q_D includes the dynamic losses at cavities and couplers. Q_{D-det} corresponds to the heat loss at input couplers. The dynamic loss at the cavity is calculated by $Q_{D-cav}=Q_D - Q_{D-det}$.

The dynamic loss measurement for the DESY cavity (Z109) is shown in Fig. 6. The cavity was operated at the field gradient of 28 MV/m. The measured Q_D and Q_{D-det} were 0.84 W and 0.09 W, respectively, which were calculated from the flow rate of evaporated LHe. The dynamic loss at the cavity, Q_{D-cav} , was calculated to be 0.75 W, corresponding to a Q_0 value was 8.8×10^9 . The measured values for the other cavities are listed in Table 4.

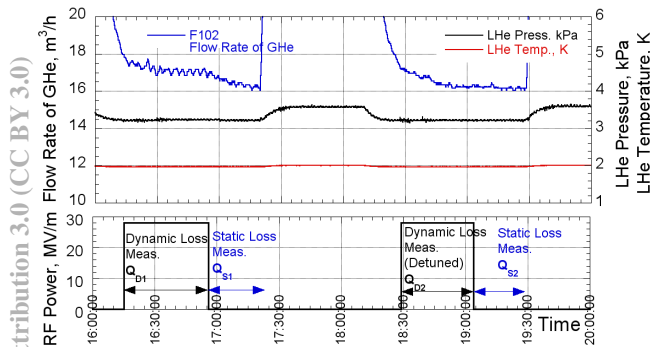


Figure 6: Thermal conditions of dynamic loss measurement.

Table 4: Measured Dynamic Loss of Single Cavity

	MC-4 Z109	MC-1 AES004	MA-3 MHI07	MA-2 MHI06	MA-2 MHI06
G , MV/m	28	25.2	32.3	38	32
Q_D , W	0.84	1.4	2.8	4.8	2.6
Q_{D-det} , W	0.09	0.18	0.7	1.8	1.2
Q_{D-cav} , W	0.75	1.3	2.0	2.9	1.3
Q_0	8.8×10^9	4.3×10^9	4.3×10^9	4.2×10^9	6.5×10^9

Dynamic Loss by Four and Seven Cavities

Dynamic loss measurements were performed with four and seven cavities. The measured losses and the average field gradient of the cavities, G_{ave} , are listed in Table 5. Four cavities in Module-C and Module-A were operated at $G_{ave} = 20$ MV/m and 26.0 MV/m, respectively, and the losses of Q_{D-cav} were 2.5 W and 4.4 W. Since one cavity in Module-C had a trouble in the frequency tuner, eight cavities were not able to be operated simultaneously. The dynamic loss at the operation of seven cavities was measured at $G_{ave} = 25.4$ MV/m, and Q_{D-cav} was 7.0 W.

In order to estimate the heat loss of the input couplers at the ILC nominal gradient, four cavities in each Module were detuned and operated at the same power level of 32 MV/m. The losses of Q_{D-det} of Module-C and A were 0.5 W and 4.6 W, respectively. The design of one TTF-III coupler is 0.06 W [4], and the measured loss of 0.5 W for four couplers agrees with this estimation. The STF-2 couplers [5] had the loss of 4.6 W, and the loss was consistent with the single cavity measurement of MHI06. From the temperature measurement, the temperature rises were found at the connection flanges between the STF-2 couplers and the cavity beam pipes, as shown in Fig. 7. The temperature rises of STF-2 couplers were about 10 K while those of TTF-III couplers were less than 1 K. This temperature rise is considered to be due to heat generation at the Cu layer of 3 μ meter thickness on the inner surface of the outer conductor. The Cu layer of STF-2 coupler will be studied and it will be improved in the next model.

Table 5: Dynamic Loss at Four and Seven Cavities

	MC 4 cav.	MC 4 cav.	MA 4 cav.	MA 4 cav.	MC-MA 7 cav.
G_{ave} , MV/m	20 (average)	32 (detune)	26.9 (average)	32 (detune)	25.4 (average)
Q_D , W	2.7	NA	6.9	NA	9.6
Q_{D-det} , W	0.2	0.5	2.5	4.6	2.6
Q_{D-cav} , W	2.5	NA	4.4	NA	7.0

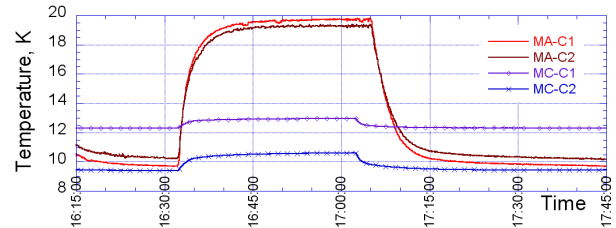


Figure 7: Temperature changes of the connection flanges of input couplers at detuned 32 MV/m. MA-C1 and C2: STF-2 couplers, MC-C1 and C2: TTF-III couplers.

CONCLUSION

The static heat loads of S1-G cryomodule were measured and compared with the design. They showed a good agreement. The dynamic loads of cavities and input couplers were measured. They will be used for the design of the ILC cryomodule and the cryogenic system.

REFERENCES

- [1] N. Ohuchi, et al, "S1-Global collaborative efforts 8-cavity-cryomodule:2 FNAL, 2 DESY and 4 KEK", LINAC'10 Tsukuba, p. 31 (2010).
- [2] E. Kako, et al, "S1-Global Module Tests at STF/KEK", in this conference, M00DA02.
- [3] C. Pagani, et al., TESLA Report 2001-36.
- [4] M. Dohlus, et al, "Tesla RF power coupler thermal calculations", LINAC 2004, Lubeck, p. 174 (2004).
- [5] E. Kako, et al, "Advances and performance of input coupler at KEK", SRF'09, Berlin, p. 485 (2009).